Available online at www.sciencedirect.com
SCIENCE DIRECT
Carbohydrate Polymers 60 (2005) 439–448
Carbohydrate Polymers
www.elsevier.com/locate/carbpol

A solid state NMR study of locust bean gum galactomannan and Konjac glucomannan gels

M.C. Vieira, A.M. Gil*

Department of Chemistry, CICECO, University of Aveiro, 3810-193 Aveiro, Portugal

Received 5 January 2005; revised 15 February 2005; accepted 21 February 2005
Available online 25 March 2005

Abstract

This paper describes a ^{13}C solid state NMR study of hydrated powders and gels of locust bean gum galactomannan-LBG and Konjac glucomannan-KGM. Changes in relative spectral intensities, cross-polarization dynamics (T_{CH}, $T_{1\rho H}$) and relaxation times (T_{1C}, T_{1H}, T_{2H}) show that hydration (0–90%) of LBG powders increases the 10^8 Hz frequency molecular motions, probably reflecting the enhanced motion of non-aggregating segments and chain ends. Slower motions (10^4–10^5 Hz) are enhanced only slightly at 90% hydration. LBG gel shows higher spatial distinction between aggregated and non-aggregated segments than the hydrated powder and relaxation times indicate higher mobility for galactose-ramified segments, compared to linear mannose segments. While the dynamics of KGM hydration is similar to that of LBG, i.e. mainly affecting fast 10^8 Hz motions, the gel is significantly more rigid. Both spectra and relaxation times show that glucose residues in KGM gel are particularly hindered, probably due to their preferential involvement in chain aggregation.

Keywords: Polysaccharide; Gel; Hydration; LBG; Konjac; Solid state NMR

1. Introduction

Locust bean gum galactomannan (LBG) and Konjac glucomannan (KGM) are polysaccharides of the mannan family widely used in the food industry as thickeners and gelling agents. LBG is a mucilage from the seed endosperm of carob tree *Ceratonia siliqua*, L. composed of a 1,4-linked β-D-mannan backbone with 1,6-linked α-D-galactose side groups making up an approximate mannose/galactose ratio of 3.0 (Dea & Morrison, 1975). This polysaccharide exhibits a block structure with a linear main chain of D-mannosyl residues named as the 'smooth region', and regions in which D-galactosyl stubs bind to the polymer backbone, named as 'hairy regions' (Fig. 1(a)) (Dea & Morrison, 1975). LBG is well known to form a gel either after several freeze/thaw cycles or from a viscous solution after standing at room temperature for 2–3 months (Dea, Morris, Rees, Welsh, Barnes, & Price, 1977; Richardson & Norton, 1998). It is believed that LBG gels result from chain aggregation between linear mannan regions and, indeed, the degree of aggregation is seen to increases as the content in galactose decreases (Dea, McCleary, & Clark, 1986). KGM is the main component of Konjac flour obtained from the tubers of *Amorphophallus konjac* C. Koch. KGM is a nonionic polysaccharide composed of β-1,4 linked D-mannose and D-glucose (mannose/glucose ratio = 1.6) with branches 11–16 residues long, occurring every 10–11 residues in the main chain (Fig. 1(b)) (Maeda, Shimahara, & Sugiyama, 1980). Monomers or short segments of mannose and glucose alternate, either in the main chain or in the ramification segments. Natural KGM is partially acetylated and forms a thermally irreversible gel by heating in the presence of an alkaline coagulant (Meakaji, 1974; Williams, Foster, Martin, Norton, Yoshimura, & Nishinari, 2000). It has been observed that deacetylation promotes aqueous insolubility of the polymer and subsequent chain aggregation, leading to the formation of a gel network (Williams, Foster, Martin, Norton, Yoshimura, & Nishinari, 2000).

A vast number of studies have been carried out to elucidate the hydration and gelation processes of these

* Corresponding author. Tel.: +351 234 370707; fax: +351 234 370084.
E-mail address: agil@dq.ua.pt (A.M. Gil).

0144-8617/$ - see front matter © 2005 Elsevier Ltd. All rights reserved.
doi:10.1016/j.carbpol.2005.02.013

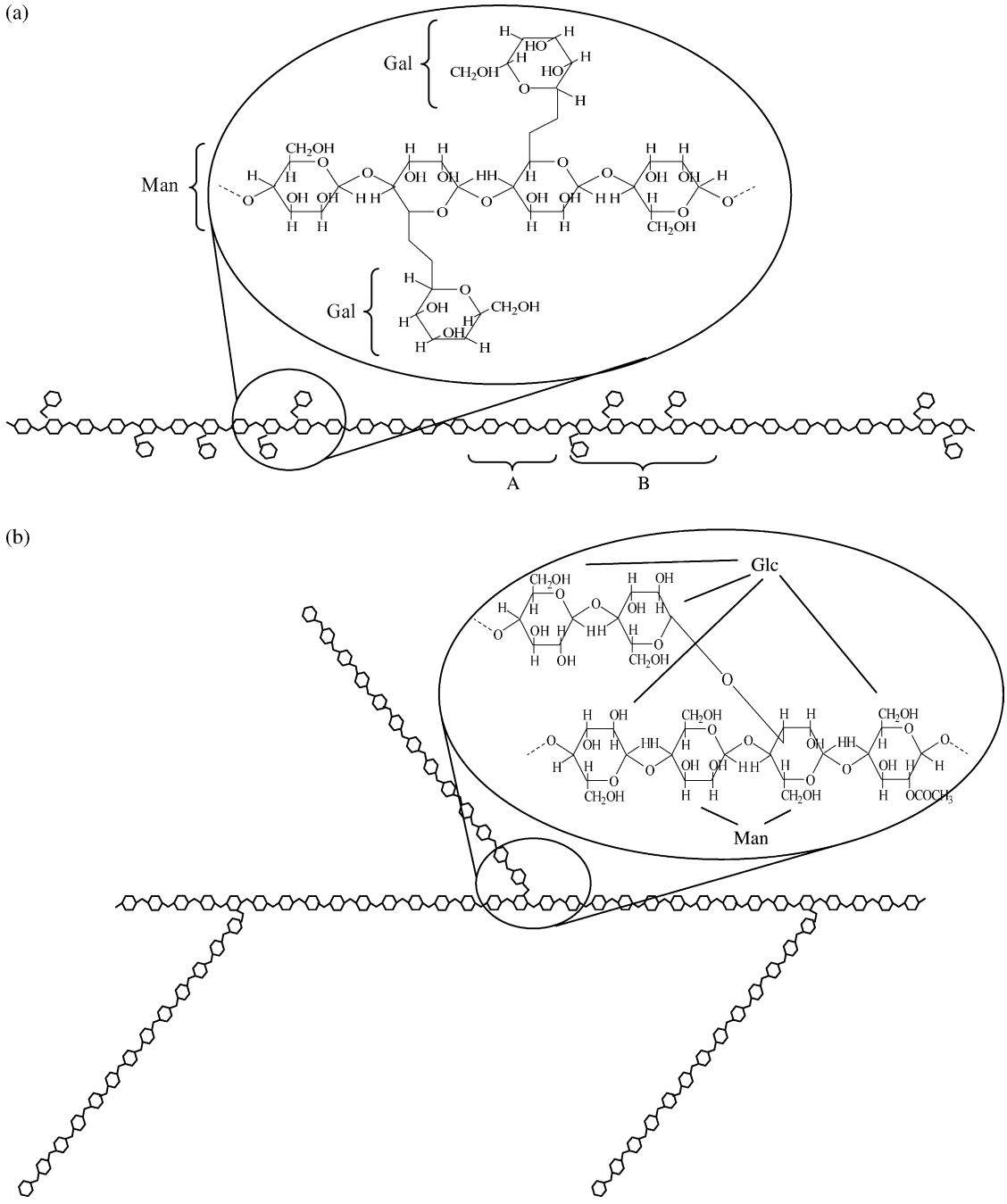

Fig. 1. Schematic representation of generally accepted structures of (a) Locust bean gum galactomannan (LBG), where A and B represent linear and ramified segments, respectively, and (b) Konjac glucomannan (KGM).

polysaccharides in view of their increasing use as industrial thickeners and stabilizers (Davé & McCarthy, 1997; Doublier & Launay, 1981; Kök, Hill, & Mitchell, 1999; Lopes da Silva & Gonçalves, 1990; Richardson & Norton, 1998; Richardson, Clark, Russel, Aymard & Norton, 1999; Williams et al., 2000; Yoshimura & Nishinari, 1999). However, to our knowledge, few studies have been concerned with the molecular level description of the corresponding gel systems. Solid state NMR is a valuable tool for the characterization of semi-solid samples such as gels and Gidley, McArthur, and Underwood, 1991 have reported a detailed solid state ^{13}C NMR study of powders, hydrates and gels of a range of galactomannans. Comparison between ^{13}C cross-polarization and magic-angle-spinning (CP/MAS) and ^{13}C single-pulse-excitation (SPE) spectra has enabled 'solid-like' and 'liquid-like' environments to be identified, respectively, in both hydrates and gels. Based on the analysis of relative intensities of the NMR peaks observed, the authors have been able to suggest that, for LBG gel, the solid-like environment involves

segments with higher mannose:galactose ratios. For the KGM gel, a similar approach suggested that intermolecular aggregation may involve segments with lower mannose:-glucose ratios. More recently, a number of reports have been published on the use of NMR spectroscopy to investigate the interaction of LBG and KGM with cellulose (Newman & Hemmingson, 1998; Whitney, Brigham, Darke, Reid, & Gidley, 1998) and algae polysaccharides (Piculell, Zhang, Turquois, Rochas, Taravel, & Williams, 1994) and a ^{1}H NMR relaxometry study of the gelation mechanism of Konjac mannan has been performed (Williams et al., 2000).

The present work describes a detailed ^{13}C solid state NMR study of the molecular structure and dynamics changes occurring upon hydration and upon gelation for both LBG and KGM polymers, in order to characterize further the molecular level properties of the gels. Powders and gels with comparable water content are thoroughly characterized by ^{13}C CP/MAS and SPE spectra, as well as by a range of relaxation time constants with the ability of probing molecular motions in different frequency ranges. CP dynamics parameters (cross polarization time constant, T_{CH}, and proton spin-lattice relaxation in the rotating frame, $T_{1\rho H}$), are sensitive to molecular density and motion, particularly at frequencies close to the spin-locking frequency, i.e. 10^4–10^5 Hz. Both proton and carbon spin-lattice relaxation times in the laboratory frame, T_{1H} and T_{1C}, are sensitive to faster motions in the range of the Larmor frequency, i.e. 10^8 Hz, but only T_{1C} probes localized motions since T_{1H} is strongly affected by spin diffusion between neighboring nuclei. Proton spin–spin relaxation times, T_{2H}, are sensitive to a range of molecular motional frequencies, often complementing the information provided by the remaining parameters.

2. Materials and methods

2.1. Sample analysis and preparation

The samples of LBG and KGM used were kindly provided by Provisco AG (Hauptwill, Switzerland) and Kyoei Konnyku Inc. (Kobe, Japan), respectively, and were used without further purification. Their neutral sugar composition was determined after hydrolysis with sulfuric acid, conversion into alditol-acetates and subsequent analysis by gas chromatography, following a method described previously (Blakeney, Harris, Henry, & Stone, 1983). LBG was found to have a mannose/galactose ratio of 3.00 and KGM was characterized by a mannose/glucose ratio of 1.60; these results are consistent with those found in literature (Dea & Morrison, 1975; Maeda, Shimahara, & Sugiyama, 1980).

For the NMR experiments, LBG and KGM powders were dried under vacuum at 40 °C until constant weight. Deuterated water (90% D_2O) was used for sample hydration in order to enable ^{1}H MAS spectra (not shown) to be recorded for selected samples. Preparation of powders with 30% (w/w) water was carried out by leaving the dry powder to equilibrate under 100% relative humidity in a sealed vessel. Hydration to 60 and 90% required mixing the polysaccharide with the corresponding quantities of deuterated water and keeping the sample in a sealed vessel for 24 h at 50 °C. Water contents were determined gravimetrically. For the preparation of the gel samples, 2.0% (w/w) aqueous solutions of each polymer were prepared and stirred at room temperature for 1 h and, at 75 °C, for a second hour. The LBG gel sample was attained by freeze-thaw treatment of the 2.0% solution, with three freeze-thaw cycles after which the gel was seen to contract significantly. For the NMR experiments on the LBG gel, the sample was concentrated by squeezing the sample and the water content of the resulting sample was found to be 96% water. The KGM gel sample was obtained by addition of 15.0% (w/w) NaOH aqueous solution to the 2.0% polymer solution until pH 12.2 was reached. Upon freeze-thaw treatment of three cycles, the deacetylated solution lead to gel formation. For the NMR experiences the KGM gel was concentrated by squeezing and the resulting water content was found to be 88% water.

2.2. NMR measurements

All ^{13}C CP/MAS and SPE NMR spectra were carried out on a Bruker AVANCE-400 (DRX) NMR spectrometer operating as 400 MHz for proton and 100 MHz for carbon, using 4 and 7 mm CP/MAS Bruker double-bearing probes. Rotors were spun at rates 5.0–7.0 kHz, as indicated in figure captions. The ^{13}C CP/MAS spectra were recorded using a proton 90° pulse length of 3.0–4.0 μs, 1 ms contact time and recycle time of 5 s. The ^{13}C SPE spectra were recorded with a recycle time of 5 s. The numbers of co-added scans are indicated in the figure captions. T_{CH} and $T_{1\rho H}$ time constants were measured by fitting the peak intensity curves resulting from variable contact time experiments using contact times in the 0.1–15 ms range. T_{1C} relaxation times were measured using the Torchia sequence (Torchia, 1978) with inter pulse delays in the 5 ms–40 s range. T_{1H} and T_{2H} relaxation times were measured through the modification of the CP/MAS pulse sequence so as to include, respectively, an inversion-recovery sequence and a spin-echo on the proton channel, prior to the CP step. Interpulse delays in the 10 ms–10 s and 1 μs–12 ms ranges were employed, respectively, for T_{1H} and T_{2H} measurements. For both gels and powders of higher hydration, rotors containing an inner bottom and top spacer were used, thus improving spinning stability and avoiding water separation effects. For the lower hydration samples, standard rotors could be used since no phase separation was observed.

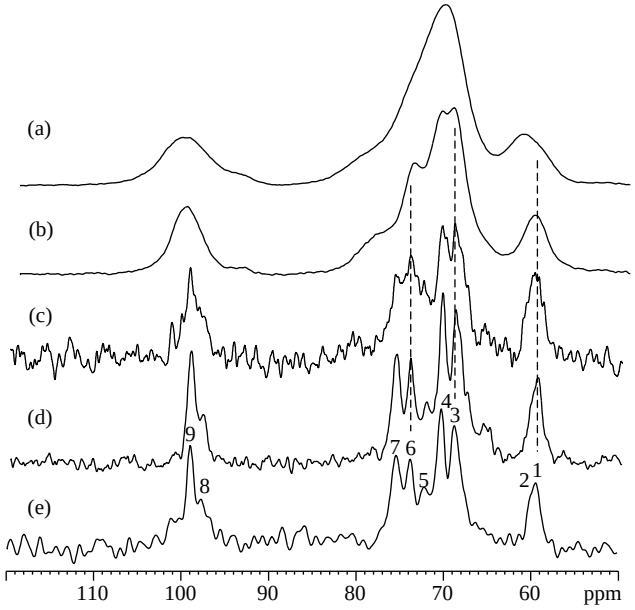

Fig. 2. ^{13}C CP/MAS spectra of LBG powder with (a) 0% (6840 scans), (b) 30% (1600 scans), (c) 60% (1600 scans) and (d) 90% (1600 scans) hydration (w/w) and e) of the gel (96% water, 2400 scans); spinning rates 6–7 kHz. Dashed lines shown to guide the eye. A 30 Hz linebroadening was applied to the spectra of hydrated powders and gel. Assignment proposed: 1: C6gal, 2: C6man, 3: C2man, 4: C5gal, 5: C3man, 6: C5man, 7: C4man, 8: C1gal, 9: C1man.

3. Results and discussion

3.1. Locust bean gum galactomannan (LBG)

Fig. 2(a–d) shows the ^{13}C CP/MAS spectra of LBG powders hydrated to different extents and Fig. 2(e) shows the spectrum of the gel sample. The level of highest hydration (90%) was chosen so as to approach as far as possible the water content of the gel (96%), in order to allow direct comparison between gel and hydrated powder.

The main effects of sample hydration are marked decrease in signal to noise ratio, due to lower sample amounts and higher mobility in hydrated samples, and marked resolution enhancement. The latter effect is expected with basis on previous work on LBG (Gidley, McArthur, & Underwood, 1991) and on similar systems such as starch or cellulose and reflects the enhanced mobility of the system by the water, allowing a narrower range of stable molecular conformations to be adopted. A broad unassigned hump, seen at about 80 ppm at 0 and 30% hydration levels, disappears for higher hydrations, probably reflecting ring resonances arising from amorphous environments. The assignments indicated in Fig. 2(e) and listed in Table 1 are suggested with basis on chemical shifts of fenugreek galactomannan (Ramesh, Yamaki, Ono, & Tsushida, 2001) and of guar gum galactomanna, both in the liquid state (Grasdalen & Painter, 1980; Noble & Taravel, 1987), as well as with basis on previous solid state NMR work on LBG (Gidley, McArthur, & Underwood, 1991). It is noted that, for LBG, no significant differences are observed between liquid state chemical shifts and those found for powders and gel. With the exception of a small shift to lower ppm of the C6 resonances, from 0 to 30% hydration, and which may reflect a small conformational change, no significant chemical shift changes are observed upon hydration, which indicates that no major conformational changes take place. Fig. 3 shows the corresponding ^{13}C SPE spectra, recorded with recycle 5 s, thus enhancing the signals from liquid-like carbon environments. Although CP/MAS and SPE spectra may not be considered exclusive, since one same environment may contribute to some extent to both types of spectra, the experimental conditions chosen (namely, short contact time and short recycle delay, in CP/MAS and SPE experiments, respectively) do lead to enhancement of signals from more hindered (or solid-like) environments in the CP/MAS experiments and, conversely, of signals from more mobile (or liquid-like) environments in the SPE experiment. Therefore, changes in relative intensities from the CP/MAS spectrum to the SPE spectrum may be interpreted with basis on distinct mobilities for different carbon environments. In the dry state, C6 carbons

Table 1
Cross-polarization time constants, T_{CH}, and proton spin-lattice relaxation times in the rotating frame, $T_{1\rho H}$, for hydrated powders and gel of Locust bean gum galactomannan (LBG)

Assignment		0% D_2O		60% D_2O		90% D_2O		Gel (96% D_2O)	
δ/ppm		T_{CH}/ms	$T_{1\rho H}$/ms	T_{CH}/ms	$T_{1\rho H}$/ms	T_{CH}/ms	$T_{1\rho H}$/ms	T_{CH}/ms	$T_{1\rho H}$/ms
C1man	100.3	0.058±0.010	14.4±3.2	0.37±0.10	19.8±4.7	0.21±0.02	9.4±0.7	0.37±0.10	8.5±1.8
C1gal	99.4			1.4±0.3	17.5±4.3	0.32±0.03	14.9±1.2	0.14±0.04	15.5±3.1
C4man	75.8			1.5±0.3	11.1±2.0	0.28±0.05	11.9±1.6	0.35±0.08	11.3±2.2
C5man	74.3			0.94±0.17	12.1±1.8	0.33±0.03	11.6±0.9	0.26±0.08	13.6±3.8
C3man	72.5					n.d.	n.d.	0.39±0.08	9.4±1.7
C5gal	70.3					0.22±0.04	11.5±1.5	0.63±0.19	10.2±3.0
C2man	69.2	0.056±0.010	13.2±2.8	1.1±0.3	17.8±5.4	0.36±0.04	15.2±1.5	0.69±0.14	18.0±4.7
C3,C4 gal	68.5			1.3±0.3	23.4±6.5	0.43±0.04	22.2±2.0		
C6man	61.0	0.041±0.007	12.4±2.0						
C6gal	59.6			0.61±0.16		0.15±0.03	15.8±2.1	0.25±0.09	8.1±2.0

The uncertainty shown for each value corresponds to that of curve fitting and calculation of each parameter. n.d.—value not determined due to poor signal to noise ratio of peak and/or large error in fitting.

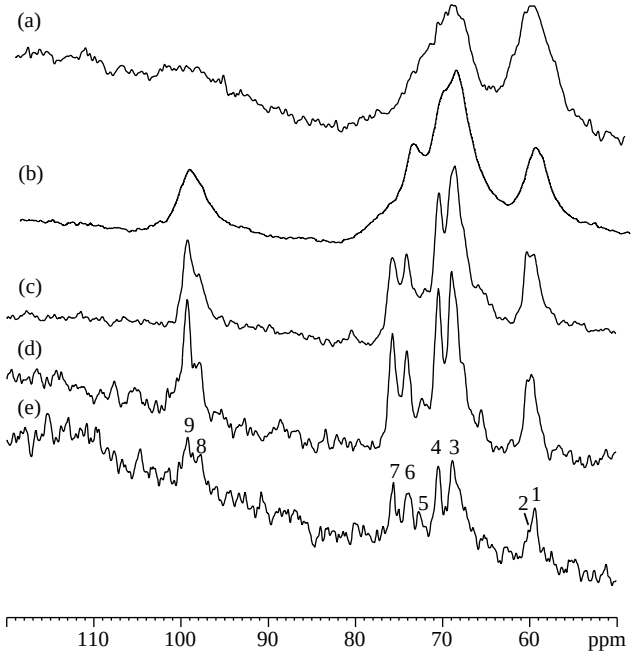

Fig. 3. ^{13}C SPE spectra of LBG powder with (a) 0% (1600 scans), (b) 30% (1800 scans), (c) 60% (500 scans) and (d) 90% (524 scans) hydration (w/w) and (e) of the gel (96% water, 2000 scans); spinning rates 6–7 kHz. The riding up effect on the baseline of some spectra is due to probe background signal. A 30 Hz linebroadening was applied to the spectra of hydrated powders and gel. Peak numbering and assignment as in Fig. 2.

and some ring carbons clearly show up in the spectra (Fig. 3(a)), indicating that such environments show considerable mobility even in the dry state. As hydration increases, all remaining carbon environments become significantly more mobile which leads to SPE spectra resolved in all regions (Fig. 3(c) and (d)). At 90% hydration, both CP/MAS and SPE spectra are generally similar, with the exception of a small difference in the C6 profile.

The CP/MAS spectra of the 90% hydrated sample and the gel are generally very similar (Fig. 2(d) and (e)), however, the SPE spectra of the two samples (Fig. 3(d) and (e)) show that, for the gel, the mannose C6 shoulder (peak 2) and mannose C1 peak (peak 9) are reduced in relative intensity, compared to the spectrum of the powder. This indicates lower average mobility of mannose residues compared to galactose residues, which is consistent with mannose-rich segments being able to aggregate more effectively in the gel, thus, becoming more motionally hindered relatively to galactose-containing ramified segments. This point will be further discussed below.

The dynamic characterization of all samples was carried out in order to help enlighten structural differences between hydrated powders and gels. Since the measurements shown are based on the observation of the ^{13}C signal, low signal to noise has in some cases hindered the calculation of time constants with adequate precision; these cases are indicated in Tables 1–5 as n.d. (not determined). Table 1 shows the CP dynamics parameters for LBG powders with 0, 60 and 90% water and for the gel. The cross polarization time constant, T_{CH}, is shown to be significantly dependent on the level of hydration. At 60% hydration, values increase 10–20 times for most peaks, reflecting the molecular mobility enhancement taking place which results in slower cross-polarization. Interestingly, all T_{CH} values drop again at 90% hydration, which may be due either to some increased rigidity in the system, e.g. due to enhanced aggregation between compatible segments, and/or to increase of water density around polymer molecules, the water protons (HOD in hydration water) contributing to higher cross polarization rates. It will be shown later that both T_{2H} and T_{1C} parameters show that molecular mobility consistently increases with hydration level, which thus suggests the water density effect as the most prominent for determining T_{CH} values at 90% hydration. $T_{1\rho H}$ values are strongly affected by spin diffusion effective within distances of few nanometers and, indeed, an average common value is observed for most carbon environments, at each hydration, and taking into account the uncertainty ranges shown (Table 1). This parameter is also a useful probe for motions of the order of the spin-locking field frequency (10^4–10^5 Hz), however, it is seen that the hydration level does not affect the average $T_{1\rho H}$ significantly for LBG, the values only hinting a slight shortening at the highest hydration. This indicates that 10^4–

Table 2
Proton and carbon spin-lattice relaxation times, T_{1H} and T_{1C}, for hydrated powders and gel of Locust bean gum galactomannan (LBG)

Assignment		0% D_2O		60% D_2O		90% D_2O		Gel (96% D_2O)	
δ/ppm		T_{1H}/s	T_{1C}/s	T_{1H}/s	T_{1C}/s	T_{1H}/s	T_{1C}/s	T_{1H}/s	T_{1C}/s
C1man	100.3	3.7±0.02	28±3.3	n.d.	0.38±0.02	n.d.	0.25±0.02	1.6±0.37	0.28±0.06
C1gal	99.4			1.3±0.01	0.31±0.09	1.1±0.11	0.26±0.04	1.5±0.34	0.34±0.07
C4man	75.8			1.6±0.01	0.30±0.02	1.1±0.11	0.23±0.02	1.1±0.23	0.22±0.02
C5man	74.3			1.4±0.01	0.39±0.05	1.2±0.27	0.26±0.02	1.2±0.18	0.30±0.07
C3man	72.5			1.4±0.01	0.46±0.05	1.2±0.35	0.26±0.03	0.87±0.13	0.25±0.08
C5gal	70.3	3.6±0.02	19±1.3	n.d.	0.32±0.03	1.1±0.04	0.21±0.02	1.2±0.21	0.21±0.04
C2man	69.2			1.4±0.01	0.39±0.02	n.d.	0.22±0.02	1.6±0.25	0.21±0.06
C3,C4 gal	68.5			n.d.	0.24±0.04	1.3±0.10	0.21±0.02	1.7±0.45	0.19±0.06
C6man	61.0	3.5±0.02	4.2±0.91		0.09±0.01		0.13±0.02	0.62±0.10	0.13±0.03
C6gal	59.6			1.3±0.01	0.14±0.02	1.3±0.18	0.13±0.02	0.74±0.17	0.14±0.03

The uncertainty shown for each value corresponds to that of curve fitting and calculation of each parameter. n.d.—value not determined due to poor signal to noise ratio of peak and/or large error in fitting.

Table 3
Proton spin–spin relaxation times, T_{2H}, for powders and gels of Locust bean gum galactomannan (LBG) and Konjac glucomannan (KGM)

		Locust bean gum galactomannan (LBG)						
Assignment		0% D_2O	60% D_2O	90% D_2O	Gel (96% D_2O)			
δ/ppm		T_{2H}/μs	T_{2H}/μs	T_{2H}/μs	T_{2HA}/μs	%A	T_{2HB}/μs	%B
C1man	100.3	27±0.02	85±0.10	129±0.11	53±5.1	71	[a]	
C1gal	99.4		140±18	115±0.11	n.d.			
C4man	75.8		141±0.12	150±0.12	16±2.7	30	275±42	70
C5man	74.3		100±0.10	192±18	20±2.4	35	575±139	65
C3man	72.5		59±6.3	132±16	9.0±1.5	32	494±95	68
C5gal	70.3	29±0.02	124±0.11	165±0.12			194±25	100
C2man	69.2		165±0.12	298±0.24			278±32	100
C3, C4 gal	68.5						365±95	100
C6man	61.0	27±0.02					181±42	100
C6gal	59.6		99±0.10	133±0.11	39±10	56	[a]	

		Konjac glucomannan (KGM)			
Assignment		0% D_2O	60% D_2O	90% D_2O	Gel (88% D_2O)
–	103.5[b]				24±3.4
C1glc	101.6	31±0.02	69±10	n.d.	17±1.7
C1man	99.1		60±8.6	138±17	26±3.7
–	81.5[b]				19±5.1
–	80.5[b]				25±5.8
C4glc	77.5		77±12	124±23	41±9.8
C4man	75.5		82±12	163±26	30±3.9
C5man, C5glc	73.9	29±0.02	103±9.7	n.d.	28±2.8
C3glc	73.1			n.d.	21±2.1
C2glc	71.9		86±8.7	210±21	20±1.5
C3man	70.6		90±16	154±40	28±1.6
C2man	69.1		112±15	314±39	26±2.1
C6man, C6glc	60.5	26±0.02	59±9.0	120±13	29±3.1

The uncertainty shown for each value corresponds to that of curve fitting and calculation of each parameter. n.d.—value not determined due to poor signal to noise ratio of peak and/or large error in fitting.
[a] Value too long to be determined with satisfactory precision.
[b] Signal only observed in the spectrum of the gel.

10^5 Hz motions, probably reflecting slower backbone motions of long chain segments, require a high hydration level in order to be enhanced. Comparison of the 90% hydrated LBG sample with the gel shows general similarity in T_{CH} and $T_{1\rho H}$ parameters (Table 1), however, for the gel some differences should be pointed out: the $T_{1\rho H}$ of galactose C6 is significantly lower compared to the remaining carbon environments and this may be due to the high mobility of the 1,6-linked α-D-galactose at the ramification points where interchain aggregation is hindered, in the gel. The mannoses directly linked to those galactose residues may also be animated with mobility higher than the mannoses comprised in the linear aggregated segments, fact which would explain the lower average $T_{1\rho H}$ value also found for mannose C1 (Table 1).

T_{1H} values are efficiently averaged out by spin diffusion up to distances of ca. 20 nm. In the dry state, a common value of about 3.6 ms is observed (Table 2), indicating that the sample is homogeneous within this distance scale. This is halved at 60% hydration due to the triggering of fast motions in the 10^8 Hz range, probably mostly reflecting motions of ramified segments and end segments, and T_{1H} is differentiated for C6 carbons by its short value due to enhanced mobility of those groups. At 90% hydration, T_{1H} values show only a slight shortening and distinction of C6 resonances is no longer seen, due to the increased uncertainties in the values at the higher hydration. T_{1C} values are not affected by spin diffusion and may, therefore, provide localized information on the MHz range dynamics. This parameter decreases two orders of magnitude from 0 to 60% hydration and, like T_{1H}, decreases only slightly further at 90%. The above results show that most mobility enhancement in terms of MHz motions occurs between 0 and 60% hydration and that increasing hydration level from 60 to 90% does not increase MHz molecular mobility significantly. In all powders, relatively short T_{1C} values are observed for the C6 resonances of both mannose and galactose monomers, indicating the expected enhanced motion of the free $-CH_2OH$ carbons relatively to the ring carbons. Overall, fast motions seem to be more affected by hydration than slower backbone motions, as viewed by the practically unchanged $T_{1\rho H}$ values. Comparing T_{1H} and T_{1C} values of the 90% hydrated powder with the gel sample (Table 2), no significant differences are noted in, which

Table 4
Cross-polarization time constants, T_{CH}, and proton spin-lattice relaxation times in the rotating frame, $T_{1\rho H}$, for hydrated powders and gel of Konjac glucomannan (KGM)

Assignment		0% D_2O		60% D_2O		90% D_2O		Gel (88% D_2O)	
δ/ppm		T_{CH}/ms	$T_{1\rho H}$/ms	T_{CH}/ms	$T_{1\rho H}$/ms	T_{CH}/ms	$T_{1\rho H}$/ms	T_{CH}/ms	$T_{1\rho H}$/ms
–	103.5[a]							0.055±0.010	6.6±1.1
C1glc	101.6	0.032±0.009	9.6±2.4	0.078±0.017	8.7±1.3	0.27±0.07	7.3±1.1	0.046±0.007	8.1±1.2
C1man	99.1			0.095±0.022	7.7±1.2	0.32±0.04	7.3±0.7	0.065±0.015	7.5±1.8
–	81.5[a]							0.050±0.015	6.7±1.7
–	80.5[a]							0.052±0.010	7.3±1.3
C4glc	77.5			0.074±0.015	10.6±1.5	0.36±0.06	14.5±2.0	0.058±0.013	7.2±1.6
C4man	75.5	0.033±0.009	9.6±2.3	0.097±0.021	9.9±1.5	0.26±0.03	12.4±1.1	0.040±0.006	11.2±1.8
C5man, C5glc	73.9			0.085±0.018	10.0±1.5	0.28±0.04	12.5±1.3	0.062±0.007	7.9±0.8
C3glc	73.1			n.d.	n.d.	0.27±0.04	11.0±1.0	0.045±0.006	8.3±1.0
C2glc	71.9			0.087±0.021	11.0±1.9	0.33±0.06	10.8±1.3	0.060±0.006	7.9±0.8
C3man	70.6			0.11±0.03	10.3±1.7	0.31±0.04	10.5±1.0	0.051±0.006	8.3±0.9
C2man	69.1			0.20±0.06	10.4±2.5	0.46±0.05	15.1±1.4	0.085±0.007	9.5±0.9
C6 man, C6 glc	60.5	0.015±0.005	9.3±2.5	0.074±0.02	8.1±1.2	0.28±0.03	6.2±0.5	0.044±0.006	6.8±0.8

The uncertainty shown for each value corresponds to that of curve fitting and calculation of each parameter. n.d.—value not determined due to poor signal to noise ratio of peak and/or large error in fitting.
[a] Signal only observed in the spectrum of the gel.

reflects similar characteristics in terms of dynamics in 10^8 Hz frequencies. This means that the dynamics of highly mobile non-aggregated ramified segments and chain ends seem to depend mostly on the water content, irrespectively of the formation of a gel network.

LBG hydration induces a gradual T_{2H} increase (Table 3), reflecting the increase in overall mobility of the system. For the dry and hydrated powder samples, all peaks show single-component T_{2H} behavior however, for the gel, bi-component behavior is observed, particularly for mannose sites. Mannose ring carbons are distributed within two dynamic populations, the more hindered of which is characterized by T_{2H} of about 10–20 μs and comprises about 30% of mannose residues. These may correspond to the linear mannose segments long enough to engage in chain aggregation, i.e. longer than 6 monomers (Dea, McCleary, & Clark, 1986). The more mobile mannose population is characterized by T_{2H} of several hundreds of μs and should correspond to non-aggregating mannose residues, located in shorter segments and in galactose-containing ramified segments. In agreement, galactose ring carbons are all characterized by very long T_{2H} values, often difficult to quantify with precision within reasonable experimental times. Interestingly, it is also observed that about half of the galactose C6 groups are significantly less mobile (T_{2HA} 39 μs), compared to galactose ring carbons (T_{2H} of several hundreds of μs). It is possible that these relatively hindered galactose CH_2OH groups belong to residues adjacent or in

Table 5
Proton and carbon spin-lattice relaxation times, T_{1H} and T_{1C}, for hydrated powders and gel of Konjac glucomannan (KGM)

Assignment		0% D_2O		60% D_2O		90% D_2O		Gel (88% D_2O)	
δ/ppm		T_{1H}/s	T_{1C}/s	T_{1H}/s	T_{1C}/s	T_{1H}/s	T_{1C}/s	T_{1H}/s	T_{1C}/s
–	103.5[a]							1.6±0.34	4.1±0.86
C1glc	101.6	3.5±0.02	18±3.2	4.1±0.6	0.39±0.08	0.99±0.13	0.21±0.06	2.0±0.10	1.7±0.35
C1man	99.1			4.2±1.1	0.31±0.07	1.2±0.14	0.13±0.02	1.9±0.30	0.56±0.11
–	81.5[a]							1.7±0.29	
–	80.5[a]							2.2±0.21	0.50±0.07
C4glc	77.5			8.4±0.9	0.18±0.06	1.1±0.11	0.59±0.11	1.8±0.48	0.44±0.05
C4man	75.5			4.4±0.9	0.18±0.06	0.91±0.08	0.17±0.02	1.8±0.19	0.41±0.04
C5man, C5glc	73.9	3.39±0.02	17±2.2	4.4±1.2	0.22±0.08	1.1±0.06	0.23±0.04	1.7±0.09	0.71±0.14
C3glc	73.1					1.1±0.06	n.d.	2.1±0.10	0.61±0.07
C2glc	71.9			3.3±0.3	0.27±0.07	1.1±0.12	0.23±0.04	2.1±0.15	0.43±0.04
C3man	70.6			4.0±0.6	0.18±0.09	1.0±0.11	0.24±0.03	1.6±0.12	0.49±0.09
C2man	69.1			3.8±0.2	0.17±0.09	1.1±0.10	0.22±0.03	1.9±0.19	0.21±0.03
C6 man, C6 glc	60.5	3.31±0.02	10±2.3	4.0±0.5	0.17±0.08	1.0±0.07	0.12±0.02	1.5±0.11	4.1±0.86

The uncertainty shown for each value corresponds to that of curve fitting and calculation of each parameter. n.d.—value not determined due to poor signal to noise ratio of peak and/or large error in fitting.
[a] Signal only observed in the spectrum of the gel.

close proximity to aggregated linear mannose segments, the mobility of galactose C6 groups being restricted by the limited backbone motion.

3.2. Konjac glucomannan (KGM)

The ^{13}C CP/MAS spectra of the hydrated powders and the gel of KGM are shown in Fig. 4. The general spectral features reproduce those reported previously for this system (Gidley, McArthur, & Underwood, 1991). The assignments suggested in the figure and Tables 3–5 were based on a recent report of the characterization of purified native KGM by liquid state NMR (Crescenzi et al., 2002) and on previous solid state NMR work on KGM (Gidley, McArthur, & Underwood, 1991). As with LBG, C6 resonances show a slight shift to lower ppm with increasing hydration, but apart from this observation, no significant chemical shift changes occur with hydration or with gelation, indicating the absence of large conformational changes. The CP/MAS spectra of KGM powders with 0 and 30% hydration (Fig. 4(a) and (b)) show broad spectral features, although some resolution enhancement and a high-field shift of the C6 peaks are noted at 30%. Hydration up to higher levels (Fig. 4(c) and (d)) has the expected effect of improving spectral resolution in all regions. The corresponding ^{13}C SPE spectra are shown in Fig. 5 indicating that all ring carbons become significantly more mobile by hydration.

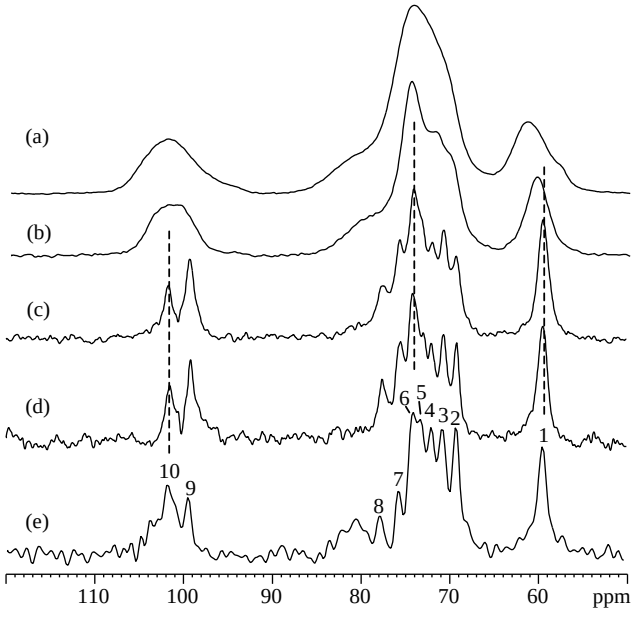

Fig. 4. ^{13}C CP/MAS spectra of KGM powder with (a) 0% (4572 scans), (b) 30% (1600 scans), (c) 60% (648 scans) and (d) 90% (1000 scans) hydration (w/w) and (e) of the gel (88% water, 1464 scans); spinning rates 5–6 kHz. Dashed lines shown to guide the eye. A 30 Hz linebroadening was applied to the spectra of hydrated powders and gel. Assignment proposed: 1: C6glc and C6man, 2: C2man, 3: C3man, 4: C2glc, 5: C3glc, 6: C5glc, 7: C4man, 8: C4glc, 9: C1man, 10: C1glc.

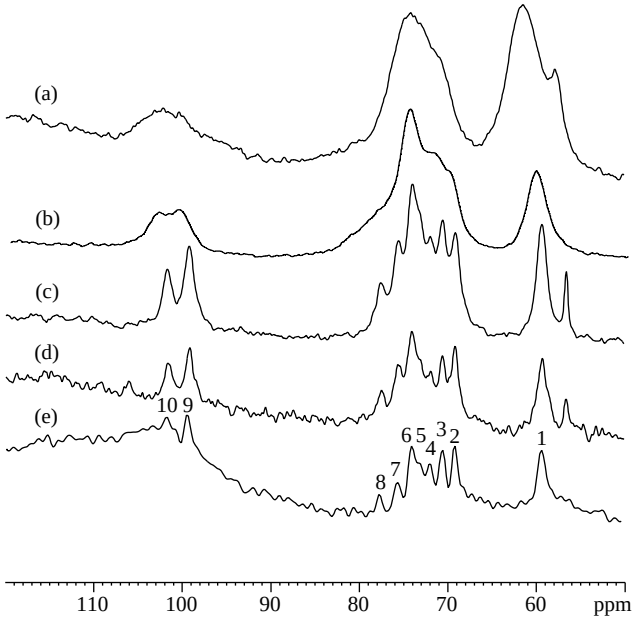

Fig. 5. ^{13}C SPE spectra of KGM powder with (a) 0% (2200 scans), (b) 30% (1800 scans), (c) 60% (540 scans) and (d) 90% (608 scans) hydration (w/w) and (e) of the gel (88% water, 1200 scans). The riding up effect on the baseline of some spectra is due to probe background signal. A 30 Hz linebroadening was applied to the spectra of hydrated powders and gel. Peak numbering and assignment as in Fig. 4.

Comparing the CP/MAS spectra of KGM gel (88% D_2O) with that of the 90% hydrated powder (Fig. 4), an intensity inversion in the C1 region is clearly seen in the gel, resulting in a mannose C1 peak weaker than that of glucose C1, in spite of the mannose/glucose ratio of 1.6 found for the KGM polymer. This suggests a relative hindrance of glucose C1 carbons in the gel. Moreover, the spectrum of KGM gel shows additional unassigned broad features at 103.5 and 81.5 and 80.5 ppm, noted before (Gidley, McArthur, & Underwood, 1991), and which seem to be characteristic of this gel. The SPE spectrum of the gel sample shows the absence of these features indicating that they arise from relatively rigid environments in the gel (Fig. 5(e)). The absence of acetyl groups due to the deacetylation treatment for the preparation of the gel is confirmed by the absence of the acetyl peak at about 20 ppm (not shown).

Hydration induces a gradual increase of T_{CH} values up to one order of magnitude at 90% water (Table 4). Interestingly, the gel (88% water) is characterized by T_{CH} values significantly shorter than those registered for the 90% hydrated powder thus indicating that the molecular arrangement in the gel is more hindered than that of the hydrated sample, in spite of the same water content in both samples. As with LBG, $T_{1\rho H}$ values do not vary significantly with hydration or gelation (Table 4),

indicating that such processes do not affect significantly chain motions of 10^4–10^5 Hz frequencies.

The effect of spin diffusion on T_{1H} values for KGM is clearly seen on Table 5, this parameter being much less affected by hydration (values are cut down to a third at 90% hydration) than the T_{1C} values found which decrease more than one order of magnitude at 90% hydration. This T_{1H} behavior, together with the short T_{CH} values seen above, is consistent with KGM powders being characterized by relatively closer packing, compared to LBG powders. This probably results from higher chain entanglement due to the longer ramification segments of KGM. In spite of this, the variations in T_{1C} values (Table 5) show that a significant increase in rapid motions in the MHz range (probably animating chain loops and ends) occurs with hydration to 60%. As for LBG, further hydration to 90% does not shorten T_{1C} values significantly. The slightly longer T_{1C} values seen for the gel, compared to the 90% hydrated powder (Table 5), confirm the relatively higher rigidity of the gel network suggested before with basis on the T_{CH} values and which now seems to affect also fast chain motions in the 10^8 Hz range. Moreover, glucose C1, C2 and C3 carbons are characterized by longer T_{1C} times (1.73 ± 0.35, 0.427 ± 0.040 and 0.607 ± 0.073, respectively) compared to the corresponding mannose sites (0.562 ± 0.11, 0.213 ± 0.027 and 0.493 ± 0.092, respectively), indicating that, in the gel, glucose units are more rigid in the frequency time scale of 10^8 Hz. This relative high rigidity of the gel is confirmed again by the significantly short T_{2H} values (Table 3), surprisingly comparable to those found in the dry state. Again, glucose C1, C2 and C3 carbons have shorter T_{2H} times compared to the remaining carbons, in agreement with T_{1C} observations and suggesting the relative hindrance of glucose residues, probably involved preferentially in interchain bonds in the gel. This is consistent with previous proposals that chain aggregation may involve segments with lower mannose:glucose ratios (14).

4. Conclusion

The ^{13}C CP/MAS and SPE spectra of LBG and KGM clearly identify solid-like and liquid-like domains in the powders and gels of both polysaccharides. In the case of LBG gel, changes in spectral relative intensities suggest higher hindrance for most mannose residues. This was further confirmed by relaxation times measurements. Gradual hydration of LBG powders causes an increase in molecular mobility mainly in the 10^8 Hz frequency range, that is, for non-aggregating mannose–galactose segments and chain ends. These motions are promoted mainly at low hydration. Motions of the order of 10^4–10^5 Hz, probably corresponding to long amplitude backbone motions are affected only slightly by hydration up to 90% water. The LBG gel was clearly differentiated from a powder hydrated to a similar level in terms of molecular dynamic properties. The gel was characterized by higher spatial distinction between aggregated and non-aggregated segments as viewed by $T_{1\rho H}$ values. In addition, dynamic characteristics differed mainly in terms of slower motions reflected by $T_{1\rho H}$ and T_{2H}. Both parameters confirmed the proposal that ramified segments comprising both mannose and galactose residues are characterized by higher mobility, compared to linear mannose segments.

While the response of KGM to hydration is rather similar to that of LBG in that mainly 10^8 Hz motions are affected, rather than the 10^4–10^5 Hz motions, the gel network is significantly more hindered than the KGM hydrated powder or than the LBG gel. Furthermore, both T_{1C} and T_{2H} parameters show that glucose residues, and particularly C1, C2 and C3 sites, are held more rigidly in the network, probably being preferentially chosen for interchain bonding. This is consistent with previous proposals that chain aggregation may involve segments with lower mannose:-glucose ratios.

Acknowledgements

The authors thank the Foundation for Science and Technology (FCT), Portugal, for funding through the POCTI/33075/QUI/2000 project. M. Vieira thanks the FCT and the FSE for funding support through the grant SFRH/BDP/5520/2001 within the III Community framework.

References

Blakeney, A. B., Harris, P. J., Henry, R. J., & Stone, B. A. (1983). A simple and rapid preparation of alditol acetates for monosaccharide analysis. *Carbohydrate Research*, *113*, 291–299.

Crescenzi, V., Skjåk-Bræk, G., Dentini, M., Masci, G., Bernadlda, M. S., Risica, D., Capitani, D., Mannina, L., & Segre, A. L. (2002). A high field NMR study of the products ensuing from Konjak glucomannan C(6)-oxidation followed by enzymatic C(5)-epimerization. *Biomacromolecules*, *3*(6), 1343–1352.

Davé, V., & McCarthy, S. P. (1997). Review of Konjac glucomannan. *Journal of Environmental Polymer Degradation*, *5*(4), 237–241.

Dea, I. C. M., McCleary, B. V., & Clark, A. H. (1986). Effect of galactose-substitution-patterns on the interaction properties of galactomannas. *Carbohydrate Research*, *147*, 275–294.

Dea, I. C. M., Morris, E. R., Rees, D. A., Welsh, E. J., Barnes, H. A., & Price, J. (1977). Associations of like and unlike polysaccharides: mechanism and specificity in galactomannans, interacting bacterial polysaccharides, and related systems. *Carbohydrate Research*, *57*, 249–272.

Dea, I. C. M., & Morrison, A. (1975). Chemistry and interactions of seed galactomannans. *Advances in Carbohydrate Chemistry and Biochemistry*, *31*, 241–312.

Doublier, J. L., & Launay, B. (1981). Rheology of galactomannan solutions: comparative study of guar gum and locust bean gum. *Journal of Texture Studies*, *12*, 151–172.

Gidley, M. J., McArtur, A. J., & Underwood, D. R. (1991). NMR characterization of molecular structures in powders, hydrates and gels

of galactomannans and glucomannans. *Food Hydrocolloids*, *5*(1/2), 129–140.

Grasdalen, H., & Painter, T. (1980). NMR studies of composition and sequence in legume-seed galactomannans. *Carbohydrate Research*, *81*, 59–66.

Kök, M. S., Hill, S. E., & Mitchell, J. R. (1999). A comparison of the rheological behaviour of crude and refined locust bean gum preparations during thermal processing. *Carbohydrate Polymers*, *38*(3), 261–265.

Lopes da Silva, J. A., & Gonçalves, M. P. (1990). Studies on a purification method for locust bean gum by precipitation with ethanol. *Food Hydrocolloids*, *4*(4), 277–287.

Maeda, M., Shimahara, H., & Sugiyama, N. (1980). Detailed examination of the branched structure of Konjac glucomannan. *Agricultural and Biological Chemistry*, *44*(2), 245–252.

Maekaji, K. (1974). The mechanism of gelation of Konjac Mannan. *Agricultural and Biological Chemistry*, *38*(2), 315–321.

Newman, R. H., & Hemmingson, J. A. (1998). Interactions between locust bean gum and cellulose characterized by ^{13}C NMR spectroscopy. *Carbohydrate Polymers*, *36*(2-3), 167–172.

Noble, O., & Taravel, F. (1987). Nuclear magnetic resonance evidence of the guarborate interaction. *Carbohydrate Research*, *166*(1), 1–11.

Piculell, L., Zhang, W., Turquois, T., Rochas, C., Taravel, F. R., & Williams, P. A. (1994). Effects of added galacto-and gluco-mannans on the NMR spectra of ^{133}Cs ions in kappa-carrageenan gels. *Carbohydrate Research*, *265*(2), 281–290.

Ramesh, H. P., Yamaki, K., Ono, H., & Tsushida, T. (2001). Two-dimensional NMR spectroscopic studies of fenugreek (*Trigonella foenum-graecum* L.) galactomannan without chemical fragmentation. *Carbohydrate Polymers*, *45*(1), 69–77.

Richardson, P. H., Clark, A. H., Russell, A. L., Aymard, P., & Norton, I. T. (1999). Galactomannan gelation: a thermal and rheological investigation analyzed using the cascade model. *Macromolecules*, *32*, 1519–1527.

Richardson, P. H., & Norton, I. T. (1998). Gelation behavior of concentrated locust bean gum solutions. *Macromolecules*, *31*, 1575–1583.

Torchia, D. A. (1978). The measurements of proton-enhance carbon-13 T_1 values by a method which suppresses artifacts. *Journal of Magnetic Resonance*, *30*, 613–616.

Whitney, S. E. C., Brigham, J. E., Darke, A. H., Reid, J. S. G., & Gidley, M. J. (1998). Structural aspects of the interaction of mannan-based polysaccharides with bacterial cellulose. *Carbohydrate Research*, *307*(3-4), 299–309.

Williams, M. A. K., Foster, T. J., Martin, D. R., Norton, I. T., Yoshimura, M., & Nishinari, K. (2000). A molecular description of the gelation mechanism of Konjac mannan. *Biomacromolecules*, *1*, 440–450.

Yoshimura, M., & Nishinari, K. (1999). Dynamic viscoelastic study on the gelation of Konjac glucomannan with different molecular weights. *Food Hydrocolloids*, *13*(3), 227–233.